Superfluid and Mott insulating phases of magnons in an easy-plane ferromagnetic insulator

January 14, 2015

A bachelor thesis by

Victor I. Dagnelie

Supervised by

Rembert A. Duine

Abstract

In this thesis we will construct a phase diagram showing the transitions to the superfluid and Mott insulating states of magnons in an easy-plane ferromagnetic insulator with an external magnetic field applied. First we transform the Hamiltonian describing this system in several ways, to explore the basic behaviour and to obtain a boundary for the superfluid phase of these magnons. We then use a mean-field approach with the Bose-Hubbard Hamiltonian, done by van Oosten *et al.*, "Quantum Phases in an Optical Lattice", *Physical Review A* **63**, 053601 (2001), to find the Mott insulating regions. Finally, we scrutinize the validity of using this Hamiltonian for our system, by showing some of the different results it yields as compared to the original spin-Hamiltonian. We conclude that the obtained phase diagram is inaccurate for low spins ($S = 2$ or lower) but significantly more reliable for high spins ($S = 6$ and higher).

Contents

1 Introduction

Phase transitions are a major physical phenomenon in daily life. We are hardly surprised to see liquid water evaporating or freezing up under the right conditions. The physical causes for such a transition are less well-known to the public; it was not until Paul Ehrenfest combined quantum mechanics and statistical physics in 1933 [1] that we had a solid theory of how various phase transition occurred. They were described as a discontinuity in some derivative of the free energy of a system, which still proves to be a useful way to describe many common transitions.

Ehrenfest did not live to see the discovery of another phase transition, namely that of liquid Helium to the superfluid state, recognized and named by Allen *et al.* [2] and Kapitza *et al.* [3] in 1937, although he could have learned of the theoretical prediction of the closely related transition of a gas of bosons to a Bose-Einstein Condensate, published by Einstein in 1925 based on correspondence with Bose [4]. This remarkable phenomenon generally occurs when a gas of bosons (particles with an integer-spin number) is cooled to just above absolute zero temperature. There can then be a macroscopic collapse of these bosons to a single quantum state, giving the system some fascinating properties.

It was not until 1995 that such a Bose-Einstein Condensate (BEC) was actually observed in the case of weak interactions [5], but since then many more observations of different gases in a BEC have been made. Even quasiparticles like magnons [6] have now been experimentally observed in a BEC. This latter instance will be important in this thesis.

1937 proved a successful year in the discovery of states of matter. Besides the earlier described superfluid state, Mott *et al.* [7], inspired by a publication earlier that year by de Boer *et al.* [8] first described the Mott insulator state, caused by electron-electron interactions. This state could also occur within the superfluid phase of certain BEC's, and hence another phase transition was born.

In the early stages of the development of quantum mechanics, many physical phenomena were revised. In 1911 the Bohr-van Leeuwen theorem [9] showed that ferromagnetism could be described by the spins of the atoms of the material, and as such was a purely quantum mechanical effect. These spins aligned themselves to each other and an external magnetic field, thus creating macroscopic magnetic properties. When in the groundstate, all spins in the material are aligned. But when the system gains energy, the spins gain some freedom in angle. To describe the mechanics of these spin angles, Felix Bloch introduced the concept of the bosonic quasiparticles called magnons [10]. We later give a more thorough explanation of magnons.

In 2001 van Oosten *et al.* [11] analytically made phase diagrams showing the transition from superfluid to Mott insulator state of ultracold bosonic atoms trapped in an optical lattice. They were successful when using a mean-field approach. The mechanics that govern these bosonic atoms can, after some transformations and approximations, also describe the behaviour of the magnons. Therefore, it is possible to make a phase diagram of magnons, showing the transitions to the superfluid state and the Mott insulating states. Constructing this diagram is the first goal of this thesis. As a second goal, we will we scrutinize the validity of the approximations made in the process, so that we can argue under which circumstances these phase diagrams are actually valid.

We start this thesis by giving a model to describe a system in which magnons

occur. We then transform and approximate the Hamiltonian of this model in several ways to create a form which is more convenient to describe the magnons. Then we calculate a boundary for which the magnons collapse to a BEC, and explore their basic behaviour within this model. We continue by comparing our Hamiltonian to that in Ref. [11], and use their calculations to make a phase diagram of the Mott insulating regions. Finally, we compare magnon expectation values from the approximated Hamiltonian (which was used to obtain the phase diagram) to those of the original exact Hamiltonian, so that we can quantify differences and argue under which circumstances the approximation yields good results.

2 Model

Before we start any calculations or attempt to make phase diagrams, we will give a brief intuitive explanation of Bose-Einstein condensates and magnons, as they are critical to understand this thesis.

2.1 Magnons

Imagine a lattice of ferromagnetic spin particles with an external magnetic field applied. In the groundstate, all spins in this lattice are aligned to the magnetic field. We see this in Fig. 1, where the spin of particle S is aligned with a magnetic field applied in the $-z$-direction. When the strength of the magnetic field decreases, these particles will gain some freedom in spin angle (as shown by the coloured cones), and will randomly choose this angle. This deviation from the direction in which the spin angle is forced by the magnetic field can be translated to the creation of a quasiparticle called a magnon. As the magnetic field continues to weaken, more magnons can be created on the same lattice site. These magnons, then, can interact with particles on neighbouring lattice sites, as shown in Fig. 1, creating a "spin wave" that propagates through the lattice. Thus, a magnon can also been seen as the quantized version of such a spin wave, a quasiparticle that reduces the spin of a particle in the direction of the magnetic field by one unit of $\hbar$.

2.2 Bose-Einstein condensates and superfluidity

Now suppose the magnetic field in this lattice is weak enough for magnons to exist. If these magnons are then cooled to close above absolute zero temperature, they will want to occupy the lowest energy state possible. Since magnons obey bosonic statistics, it is possible for more magnons to occupy the exact same quantum state. Thus, when cooled enough, a macroscopic amount of magnons can actually condense to the same single-particle groundstate. All these magnons are then delocalized, "smeared out" over the lattice if you will, governed by the same quantum wave function. Therefore, the spin angle that was randomly chosen by the spin particles (the arrows on the cones of Fig. 1), is then aligned for all these particles by the magnon condensate, as is shown in Fig. 2. Viscosity is not applicable to such a condensate of magnons, and this property is called superfluidity.
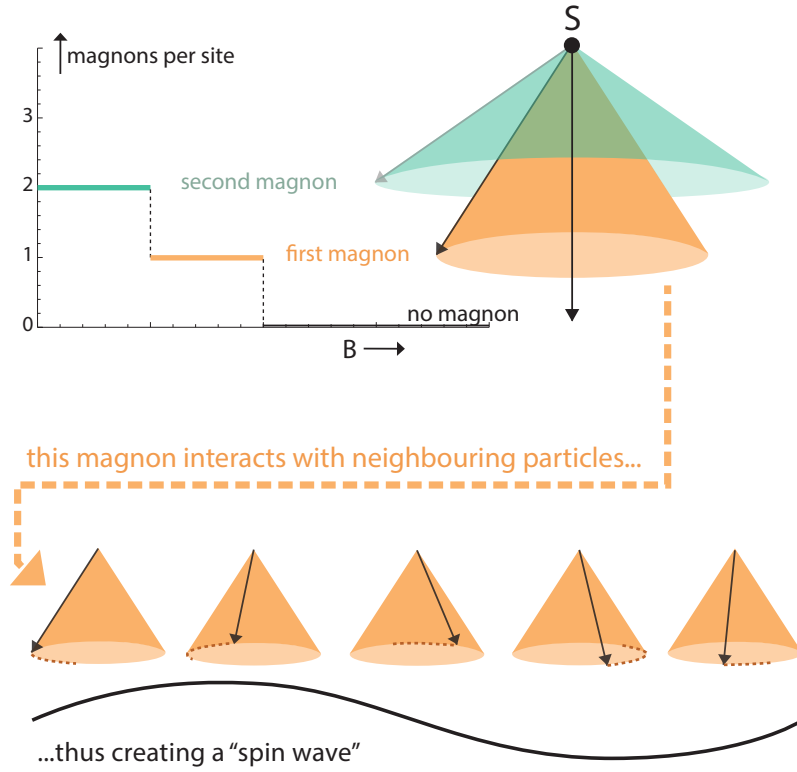
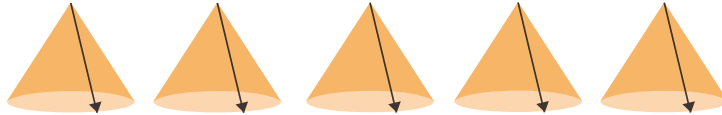Figure 1: Creation of magnons in a ferromagnetic lattice

Figure 2: Alignment of magnons in a BEC

2.3 Holstein-Primakoff transformation

Throughout this lattice we consider an easy-plane ferromagnetic insulator, i.e., a three dimensional lattice of spin particles with an external magnetic field B applied in the $-z$ direction, described by the Hamiltonian:

$$H = -\frac{J}{2\hbar^2} \sum_{\langle i,j \rangle} \vec{S}_i \cdot \vec{S}_j + \frac{K}{2\hbar^2} \sum_i (S_i^z)^2 + \frac{B}{\hbar} \sum_i S_i^z \ . \tag{1}$$

Here i and j are positions on the lattice, and $\langle i,j \rangle$ denotes a neighbouring pair of spins. Furthermore, $J > 0$ and $K > 0$ are interaction energies between sites and per site, respectively.

From this expression it is not immediately apparent in what manner we

5

are dealing with magnons. Thus, to study the behaviour of magnons in this system we first make them explicitly appear in this Hamiltonian. We do this by using the Holstein-Primakoff transformation, which is a mapping from angular momentum operators to bosonic creation and annihilation operators [12]. In our case then, it transforms the spin operators to the operators that create and annihilate magnons, as is shown in Fig. 1 by the transformation of the spin cones to explicitly created magnons. The Holstein-Primakoff transformation states:

$$
\begin{aligned}
S_i^+ &= S_i^x + iS_i^y = \hbar a_i^\dagger \sqrt{2S - a_i^\dagger a_i} \ , \\
S_i^- &= S_i^x - iS_i^y = \hbar a_i \sqrt{2S - a_i^\dagger a_i} \ , \\
S_i^z &= \hbar(a_i^\dagger a_i - S) \ ,
\end{aligned}
\tag{2}
$$

where $a_i^\dagger$ and a_i obey the commutation relation $[a_i, a_j^\dagger] = \delta_{i,j}$. These operators are related to the amount of magnons per lattice site n in our system, by $n = a_i^\dagger a_i$. Thus, magnons can explicitly be introduced in our Hamiltonian, which transforms the canonical system to an effective grand canonical one. To do so, we first note that

$$
\begin{aligned}
S_i^+ S_j^- &= S_i^x S_j^x - iS_i^x S_j^y + iS_i^y S_j^x + S_i^y S_j^y \ , \\
S_i^- S_j^+ &= S_i^x S_j^x + iS_i^x S_j^y - iS_i^y S_j^x + S_i^y S_j^y \ ,
\end{aligned}
\tag{3}
$$

so that the Hamiltonian can be written in terms of S_i^+, S_i^-:

$$
H = -\frac{J}{2\hbar^2} \sum_{\langle i,j \rangle} \left(\frac{1}{2}(S_i^+ S_j^- + S_i^- S_j^+) + S_i^z S_j^z \right) + \frac{K}{2\hbar^2} \sum_i (S_i^z)^2 + \frac{B}{\hbar} \sum_i S_i^z \ . \tag{4}
$$

The expressions for S_i^+ and S_i^- must be simplified before we can substitute them in the above Hamiltonian, otherwise we are left with too many complicated terms that will make analytical evaluation in the next chapters all but impossible. Therefore we rewrite

$$
\begin{aligned}
S_i^+ &= \hbar a_i^\dagger \sqrt{2S} \sqrt{1 - \frac{a_i^\dagger a_i}{2S}} \ , \\
S_i^- &= \hbar a_i \sqrt{2S} \sqrt{1 - \frac{a_i^\dagger a_i}{2S}} \ ,
\end{aligned}
\tag{5}
$$

so that this expression is easily simplified by using a Taylor expansion. First order expansion in powers of $1/S$ yields

$$
\begin{aligned}
S_i^+ &= \hbar a_i^\dagger \sqrt{2S} \ , \\
S_i^- &= \hbar a_i \sqrt{2S} \ .
\end{aligned}
\tag{6}
$$

This expansion is accurate when S is large. But we have to be careful here. Before we approximated this expression it could be seen that per lattice site, a state with more than $2S$ magnons would be unphysical, since then the expression in square root would become negative and hence imaginary. This observation is lost after this first order expansion, so we will have to keep it in mind. When we insert the truncated expansion into our Hamiltonian we obtain:

$$H \approx -\frac{J}{2\hbar^2} \sum_{\langle i,j \rangle} (\frac{1}{2}(2S\hbar^2 a_i^\dagger a_j + 2S\hbar^2 a_i a_j^\dagger) + \hbar^2 (a_i^\dagger a_i - S)(a_j^\dagger a_j - S))$$

$$+ \frac{K}{2\hbar^2} \sum_i \hbar^2 (a_i^\dagger a_i - S)^2 + \frac{B}{\hbar} \sum_i \hbar(a_i^\dagger a_i - S)$$

$$= -\frac{J}{2} \sum_{\langle i,j \rangle} (S(a_i^\dagger a_j + a_i a_j^\dagger) + a_i^\dagger a_i a_j^\dagger a_j - S(a_i^\dagger a_i + a_j^\dagger a_j) + S^2)$$

$$+ \frac{K}{2} \sum_i ((a_i^\dagger a_i)^2 - 2S a_i^\dagger a_i + S^2) + B \sum_i a_i^\dagger a_i - S$$

$$= -\frac{J}{2} \sum_{\langle i,j \rangle} (2S(a_i^\dagger a_j - a_i^\dagger a_i) + a_i^\dagger a_i a_j^\dagger a_j) + \frac{K}{2} \sum_i (-2S a_i^\dagger a_i + a_i^\dagger a_i a_i^\dagger a_i) + B \sum_i a_i^\dagger a_i$$

$$+ \frac{K N_s S^2}{2} - \frac{J N_s (N_s - 1) S^2}{2} - B N_s S \ ,$$

$$(7)$$

where N_s denotes the total number of lattice sites. Neglecting the constant terms and and reordering the operators and terms leaves us with the Bose-Hubbard Hamiltonian:

$$H = -\frac{J}{2} \sum_{\langle i,j \rangle} (2S a_i^\dagger a_j + a_i^\dagger a_j^\dagger a_i a_j) + (\frac{K}{2}(1 - 2S) + B + \frac{JSz}{2}) \sum_i a_i^\dagger a_i + \frac{K}{2} \sum_i a_i^\dagger a_i^\dagger a_i a_i,$$

$$(8)$$

where z is the coordination number denoting the amount of nearest-neigbours per lattice site.

2.4 Fourier transformation

In the Bose-Hubbard Hamiltonian we obtained, we consider magnons by their position on specific lattice sites and pairs of lattice sites, then summing over them to describe our entire lattice. This may not always be useful. We will also want to consider magnons by their energy, then describing the entire system by summing overall possible energies. When constructing the first phase diagram, it will become obvious why describing the Hamiltonian this way simplifies our calculations.

The energy of a magnon is related to its momentum, and we relate position and momentum by using a Fourier transformation. Thus, we Fourier transform the creation and annihilation operators using

$$a_i^\dagger = \frac{1}{\sqrt{N}} \sum_{\vec{k}} e^{-i\vec{k}\cdot\vec{x}_i} a_{\vec{k}}^\dagger \ , \qquad a_i = \frac{1}{\sqrt{N}} \sum_{\vec{k}} e^{i\vec{k}\cdot\vec{x}_i} a_{\vec{k}} \ , \qquad (9)$$

Here, $\vec{k}$ is the three dimensional wave vector and $\vec{x}_i$ a three dimensional vector denoting the location of lattice site i. We choose out lattice to lie in the cartesian x, y, z-plane and thus $\vec{k} = k_x \hat{x} + k_y \hat{y} + k_z \hat{z}$ and $\vec{x}_i = l_i a\hat{x} + m_i a\hat{y} + n_i a\hat{z}$, where a is the lattice constant and l, m, n are integers, so that $\vec{x}_i$ gives indeed all possible locations of our lattice sites.

Now we calculate the different components of our Hamiltonian. When carrying out a summation over lattice site pairs $\langle i,j \rangle$, we note that we can write this as a summation over single sites i by describing their neighbouring lattice sites j as either $i+1$ or $i-1$. Since site i has two of these neighbouring sites in every of the three dimensions we consider, we obtain six pairs per lattice sites. Dividing by 2 to avoid double-counting of these pairs we obtain:

$$
\sum_{\langle i,j \rangle} a_i^\dagger a_j = \sum_i a_i^\dagger (a_{i+1} + a_{i-1})
$$

$$
= \frac{1}{2N} \sum_{l,m,n} \sum_{\vec{k},\vec{k}'} a_{\vec{k}'}^\dagger a_{\vec{k}} e^{-i(k_x l a + k_y m a + k_z n a)}
$$

$$
[e^{i(k_x'(l+1)a + k_y' m a + k_z' n a)} + e^{i(k_x' l a + k_y'(m+1)a + k_z' n a)} + e^{i(k_x' l a + k_y' m a + k_z'(n+1)a)}
$$

$$
+ e^{i(k_x'(l-1)a + k_y' m a + k_z' n a)} + e^{i(k_x' l a + k_y'(m-1)a + k_z' n a)} + e^{i(k_x' l a + k_y' m a + k_z'(n-1)a)}]
$$

$$
= \frac{1}{2N} \sum_{l,m,n} \sum_{\vec{k},\vec{k}'} a_{\vec{k}'}^\dagger a_{\vec{k}} e^{ila(k_x'-k_x)} e^{ima(k_y'-k_y)} e^{ina(k_z'-k_z)}
$$

$$
[e^{ik_x' a} + e^{-ik_x' a} + e^{ik_y' a} + e^{-ik_y' a} + e^{ik_z' a} + e^{-ik_z' a}]
$$

$$
= \frac{1}{2} \sum_{\vec{k},\vec{k}'} a_{\vec{k}'}^\dagger a_{\vec{k}} \delta_{\vec{k},\vec{k}'} [e^{ik_x' a} + e^{-ik_x' a} + e^{ik_y' a} + e^{-ik_y' a} + e^{ik_z' a} + e^{-ik_z' a}]
$$

$$
= \sum_{\vec{k}} a_{\vec{k}}^\dagger a_{\vec{k}} [cos(k_x a) + cos(k_y a) + cos(k_z a)] \,,
$$

(10)

where we used the relation $\sum_{l,m,n} e^{ila(k_x'-k_x)} e^{ima(k_y'-k_y)} e^{ina(k_z'-k_z)} = N \delta_{\vec{k},\vec{k}'}$. Similarly we obtain the results

$$
\sum_{\langle i,j \rangle} a_i^\dagger a_i = 3 \sum_{\vec{k}} a_{\vec{k}}^\dagger a_{\vec{k}}
$$

$$
\sum_i a_i^\dagger a_i = \sum_{\vec{k}} a_{\vec{k}}^\dagger a_{\vec{k}}
$$

$$
\sum_i a_i^\dagger a_i^\dagger a_i a_i = \frac{1}{2} \sum_{\vec{k},\vec{k}',\vec{k}'',\vec{k}'''} a_{\vec{k}}^\dagger a_{\vec{k}'}^\dagger a_{\vec{k}''} a_{\vec{k}'''} \; \delta_{\vec{k}''+\vec{k}''',\vec{k}+\vec{k}'}
$$

(11)

$$
\sum_{\langle i,j \rangle} a_i^\dagger a_j^\dagger a_i a_j = \frac{1}{2} \sum_{\vec{k},\vec{k}',\vec{k}'',\vec{k}'''} a_{\vec{k}}^\dagger a_{\vec{k}'}^\dagger a_{\vec{k}''} a_{\vec{k}'''} \; \delta_{\vec{k}''+\vec{k}''',\vec{k}+\vec{k}'}
$$

$$
\times [cos(k_x' a) + cos(k_y' a) + cos(k_z' a) + cos(k_x''' a) + cos(k_y''' a) + cos(k_z''' a)] \,,
$$

so that now we can rewrite Eq. (8) in terms of $a_{\vec{k}}^\dagger, a_{\vec{k}}$:

$$
H = \sum_{\vec{k}} (\hbar\omega_{\vec{k}} + \frac{K}{2}(1-2S) + B) a_{\vec{k}}^\dagger a_{\vec{k}} + \sum_{\vec{k},\vec{k}',\vec{k}'',\vec{k}'''} \hbar\omega_{\vec{k}}' \; \delta_{\vec{k}''+\vec{k}''',\vec{k}+\vec{k}'} \; a_{\vec{k}}^\dagger a_{\vec{k}'}^\dagger a_{\vec{k}''} a_{\vec{k}'''} \,,
$$

(12)

where $\hbar\omega_{\vec{k}} = cos(k_x a) + cos(k_y a) + cos(k_z a) - 3$
and $\hbar\omega_{\vec{k}}' = cos(k_x' a) + cos(k_y' a) + cos(k_z' a) + cos(k_x''' a) + cos(k_y''' a) + cos(k_z''' a) + \frac{1}{2}$.

Let's discuss what this expression tells us. First of all, we've gone through some effort to express our Hamiltonian in terms of $a_{\vec{k}}^{\dagger}a_{\vec{k}}$. This is useful, since $\langle a_{\vec{k}}^{\dagger}a_{\vec{k}}\rangle$ is interpreted as the amount of magnons in our lattice with wave number $\vec{k}$. Thus we now have an expression that will lead to easily physically interpretable results.

The J-term in our Hamiltonian controls particle interactions between sites. It "forces" magnons to propagate, or "hop" through the lattice. When J is large compared to K, a delocalized wavefunction minimizes the magnon energy. Therefore, the system collapses to a Bose-Einstein condensate (if the usual BEC requirements are satisfied). These delocalized magnons then align the freedom in spin angle of the particles in the lattice (as shown in Fig. 2).

The K-term describes magnon-magnon interaction per site. When K is large compared to J, the energy of the system is minimized when all the sites contain the same amount of magnons. Thus in this state, no magnons will hop from one site to another, and the freedom in spin angle remains unaligned. This is shown in Fig. 3. An existing BEC of the magnons would be destroyed. This state is called the Mott insulating state.
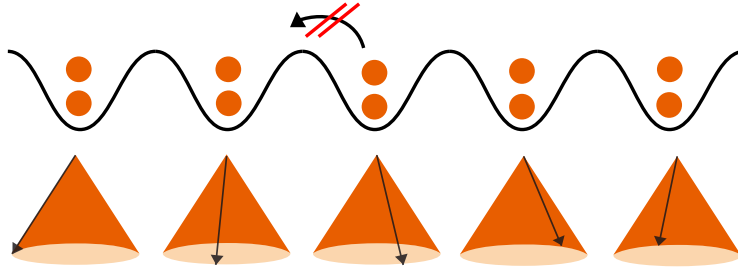

Figure 3: Mott insulating state of magnons in a lattice

However, if the amount of magnons cannot be distributed equally among lattice sites, e.g. there is a surplus of one or more magnons, the total energy of the system is equal for several magnon configurations. Then there is nothing stopping these magnons from propagating through the lattice, as is shown in Fig. 4. These magnons will become a delocalized BEC again, thus aligning the freedom in spin angle of all the particles in the lattice.
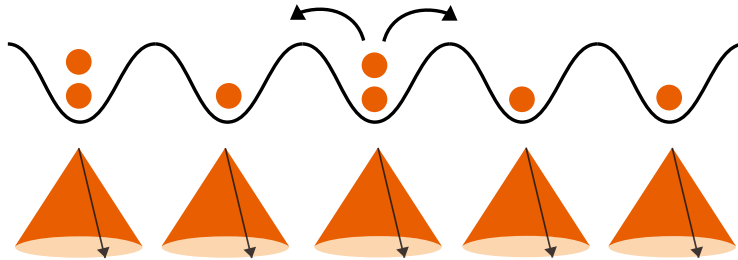

Figure 4: Possible BEC of magnons in a lattice

In the following sections we will construct phase diagrams to show the transitions between these states.

3 Basic behaviour near phase transition

Now that we have rewritten our Hamiltonian to the from of Eq. (12), we are all set to explore the behaviour of the magnons in our system. In each section we neglect some term(s) of the Hamiltonian so that a different aspect of the system can be highlighted. We discuss results to gain insight in our system and the approximations made.

3.1 Neglecting 4th order interaction terms: a superfluid boundary

We start by constructing a first phase diagram of our system. To do so, we throw away the fourth order terms in our Hamiltonian (interactions on-site and between sites) so that we are left with just

$$H = \sum_{\vec{k}} (\hbar\omega_{\vec{k}} + \frac{K}{2}(1 - 2S) + B)a_{\vec{k}}^{\dagger}a_{\vec{k}} \ . \tag{13}$$

A phase diagram is obtained by laying proper restrictions on the chemical potential μ of the system. However, in our system of magnons it is not immediately apparent what the chemical potential actually is. Therefore, we need to find its distribution function and make a comparison with the Bose-Einstein distribution function. We note that Eq. (13) can be rewritten as

$$H = \sum_{\vec{k}} \Omega_{\vec{k}} a_{\vec{k}}^{\dagger}, a_{\vec{k}} \ , \tag{14}$$

where $\Omega_{\vec{k}} = \hbar\omega_{\vec{k}} + \frac{K}{2}(1-2S) + B$. We see that this is actually a sum over many harmonic oscillators with frequencies $\Omega_{\vec{k}}/\hbar$, so that the energy states $\epsilon_{\{n_{\vec{k}}\}}$ of our system are

$$\epsilon_{\{n_{\vec{k}}\}} = \sum_{\vec{k}} \Omega_{\vec{k}}(n_{\vec{k}} + \frac{1}{2}) \ . \tag{15}$$

Here $n_{\vec{k}}$ are integers denoting the energy level, and from now on we leave out the constant term $\frac{1}{2}$. We then calculate the partition function of our system:

$$\mathrm{Z} = \sum_{\{n_{\vec{k}}\}} e^{-\beta\epsilon_{\{n_{\vec{k}}\}}} = \sum_{\{n_{\vec{k}}\}} e^{-\beta\sum_{\vec{k}}\Omega_{\vec{k}}n_{\vec{k}}} = \prod_{\vec{k}}\sum_{n}(e^{-\beta\Omega_{\vec{k}}})^{n} = \prod_{\vec{k}}\frac{1}{1 - e^{-\beta\Omega_{\vec{k}}}} \ , \tag{16}$$

so that the average energy of our system is

$$\langle U \rangle = -\frac{\partial}{\partial\beta}\ln(\mathrm{Z}) = -\frac{\partial}{\partial\beta}\ln(\prod_{\vec{k}}\frac{1}{1 - e^{-\beta\Omega_{\vec{k}}}}) = -\frac{\partial}{\partial\beta}(\sum_{\vec{k}}\ln(\frac{1}{1 - e^{-\beta\Omega_{\vec{k}}}}))$$

$$= \sum_{\vec{k}}\Omega_{\vec{k}}e^{-\beta\Omega_{\vec{k}}}\frac{1 - e^{-\beta\Omega_{\vec{k}}}}{(1 - e^{-\beta\Omega_{\vec{k}}})^{2}} = \sum_{\vec{k}}\frac{\Omega_{\vec{k}}e^{-\beta\Omega_{\vec{k}}}}{1 - e^{-\beta\Omega_{\vec{k}}}} = \sum_{\vec{k}}\frac{\Omega_{\vec{k}}}{e^{\beta\Omega_{\vec{k}}} - 1} \ . \tag{17}$$

Since the distribution function $\langle N_{\vec{k}} \rangle$ of a system is by definition related to its average energy by $\langle U \rangle = \sum_{\vec{k}} \langle N_{\vec{k}} \rangle \Omega_{\vec{k}}$, we see that the distribution function of our system is given by

$$\langle N_{\vec{k}} \rangle = (e^{\beta \Omega_{\vec{k}}} - 1)^{-1} = (e^{\beta(\hbar \omega_{\vec{k}} + \frac{K}{2}(1-2S)+B)} - 1)^{-1} \ . \tag{18}$$

Finally, comparing this to the Bose-Einstein distribution function $f(\epsilon_{\vec{k}}) = (e^{\beta(\epsilon_{\vec{k}} - \mu)} - 1)^{-1}$, we make the comparison $\epsilon_{\vec{k}} = \hbar \omega_{\vec{k}}$ and $\mu = \frac{K}{2}(2S-1) - B$.

This comparison is useful, since we know which restrictions on the chemical potential of a regular bosonic system obeying the Bose-Einstein distribution are necessary in order to reach Bose-Einstein condensation. This chemical potential should be lesser than or equal to the lowest single-particle groundstate energy, which in our case is 0 (minimum value of $\hbar \omega_{\vec{k}}$). We see that

$$\mu \begin{cases} \geq 0 & \text{if } \frac{B}{K} \leq \frac{1}{2}(2S-1) \implies \text{BEC} \\ < 0 & \text{if } \frac{B}{K} > \frac{1}{2}(2S-1) \implies \text{No BEC} \ . \end{cases} \tag{19}$$

Plotting this boundary we make our first phase diagram in Fig. 5, where we shaded our BEC phase.
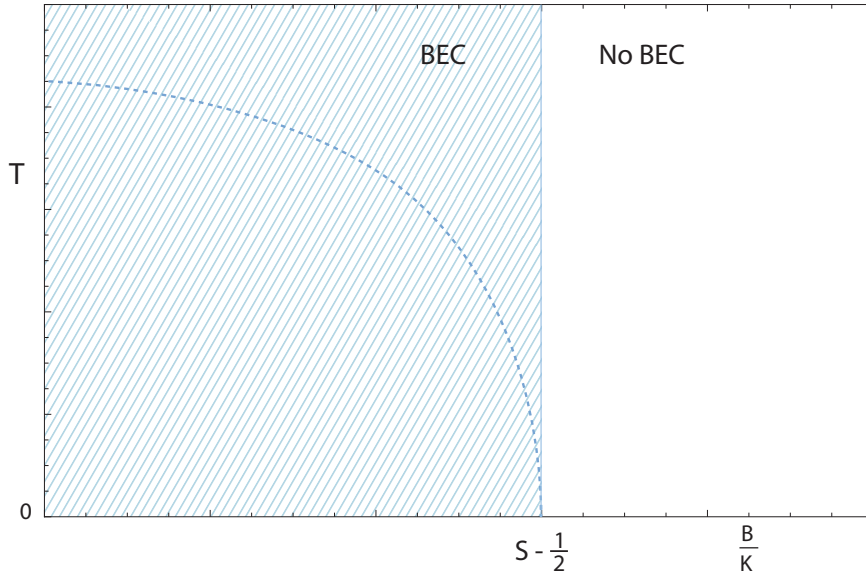

Figure 5: Superfluid boundary when neglecting magnon-magnon interactions (shaded surface), and when not neglecting them (dashed line)

This crude phase diagram is evidently independent of temperature. Once $\frac{B}{K}$ passes the threshold $\frac{1}{2}(2S-1) = S - \frac{1}{2}$, the system will collapse to a Bose-Einstein condensate. We thus have shown the interesting phenomenon that in our lattice, by varying the applied magnetic field, it seems that we can incur BEC. However, we have neglected all on-site magnon-magnon interactions, and as is discussed by Stoof $et\ al.$ [13], this does indeed leave us with this superfluid boundary which is independent of temperature. When these interactions are

not neglected, as Ref. [13] shows, one will actually find a boundary that is qualitatively shown in Fig. 5 by the dashed blue line. We keep this in mind but do not precisely calculate this curved boundary in this thesis. For temperatures close to zero our threshold at $\frac{B}{K} = S - \frac{1}{2}$ is a reasonable approximation.

3.2 Neglecting interactions between sites: a single spin problem

We saw that for the previous approximations our system would collapse to a Bose-Einstein condensate once a certain threshold of $\frac{B}{K}$ was passed, independent of temperature. We discussed however, that this is a result of having neglected the on-site magnon-magnon interactions. Clearly, to find more detail of the dynamics of our system, these interactions have to be included in our calculations. Therefore we will now describe our lattice in the case that $J = 0$, so that there are no interactions between different lattice sites. This way, every site is uncoupled, so we can just describe our system by considering a single site, then multiplying the results by N_s. Although we lose the information on magnon propagation between sites by considering this single spin, this leaves the on-site magnon-magnon interaction undisturbed by approximations.

A single lattice site is governed by the Hamiltonian

$$H = \frac{K}{2\hbar^2}(S^z)^2 + \frac{B}{\hbar}S^z \ . \tag{20}$$

Let's first consider $T = 0$. We know the eigenvalue equation

$$S_z|S, m_s\rangle = \hbar|S, m_s\rangle \quad , \text{ so } \quad H|S, m_s\rangle = (\frac{K}{2}(m_s)^2 + Bm_s)|S, m_s\rangle \ , \tag{21}$$

where m_s is the well-known secondary quantum spin number, ranging with integer steps from $-S$ to S.

We want to find the expectation value of S_z: $\langle S_z \rangle_{T=0} = \langle \Psi_{gs}|S_z|\Psi_{gs}\rangle = \hbar m_{s,\Psi_{gs}}$, where $|\Psi_{gs}\rangle$ denotes the groundstate of our system. We are thus left with the task to find the groundstate of the system and its corresponding value of m_s, so that we can evaluate $\langle S_z \rangle_{T=0}$. This groundstate however, is different in several domains of B, for different values of m_s. We check the possible eigenvalues for $S = 1$ and $S = 2$. Since we want to plot over the variable $\frac{B}{K}$ again, we divide these eigenvalues by K, and then select the groundstates depending on the domain of $\frac{B}{K}$.

Table 1: Eigenvalues for $S = 1$, divided by k

$\frac{B}{K}$	0	$(0, \frac{1}{2})$	$\frac{1}{2}$	$> \frac{1}{2}$
$m_s = -1$	$\frac{1}{2}$	$\frac{1}{2} - \frac{B}{K}$	0	$\frac{1}{2} - \frac{B}{K}$
$m_s = 0$	0	0	0	0
$m_s = 1$	$\frac{1}{2}$	$\frac{1}{2} + \frac{B}{K}$	1	$\frac{1}{2} + \frac{B}{K}$

Table 2: Eigenvalues for $S = 2$, divided by k

$\frac{B}{K}$	0	$(0, \frac{1}{2})$	$\frac{1}{2}$	$(\frac{1}{2}, 1)$	1	$(1, \frac{3}{2})$	$\frac{3}{2}$	$> \frac{3}{2}$
$m_s = -2$	2	$2 - 2\frac{B}{K}$	1	$2 - 2\frac{B}{K}$	0	$2 - 2\frac{B}{K}$	-1	$2 - 2\frac{B}{K}$
$m_s = -1$	$\frac{1}{2}$	$\frac{1}{2} - \frac{B}{K}$	0	$\frac{1}{2} - \frac{B}{K}$	$-\frac{1}{2}$	$\frac{1}{2} - \frac{B}{K}$	-1	$\frac{1}{2} - \frac{B}{K}$
$m_s = 0$	0	0	0	0	0	0	0	0
$m_s = 1$	$\frac{1}{2}$	$\frac{1}{2} + \frac{B}{K}$	1	$\frac{1}{2} + \frac{B}{K}$	$\frac{3}{2}$	$\frac{1}{2} + \frac{B}{K}$	2	$\frac{1}{2} + \frac{B}{K}$
$m_s = 2$	2	$2 + 2\frac{B}{K}$	3	$2 + 2\frac{B}{K}$	4	$2 + 2\frac{B}{K}$	5	$2 + 2\frac{B}{K}$

In Table 1 and Table 2 we highlighted the minimum values within each domain. We now know the groundstates in each domain with their respective values of m_s , so we can evaluate $\langle S_z \rangle_{T=0}$ within these domains. Finally, we conduct the Holstein-Primakoff transformation $S_z = \hbar(a^\dagger a - S)$, so

$$\langle a^\dagger a \rangle = \frac{\langle S_z \rangle}{\hbar} + S \ . \tag{22}$$

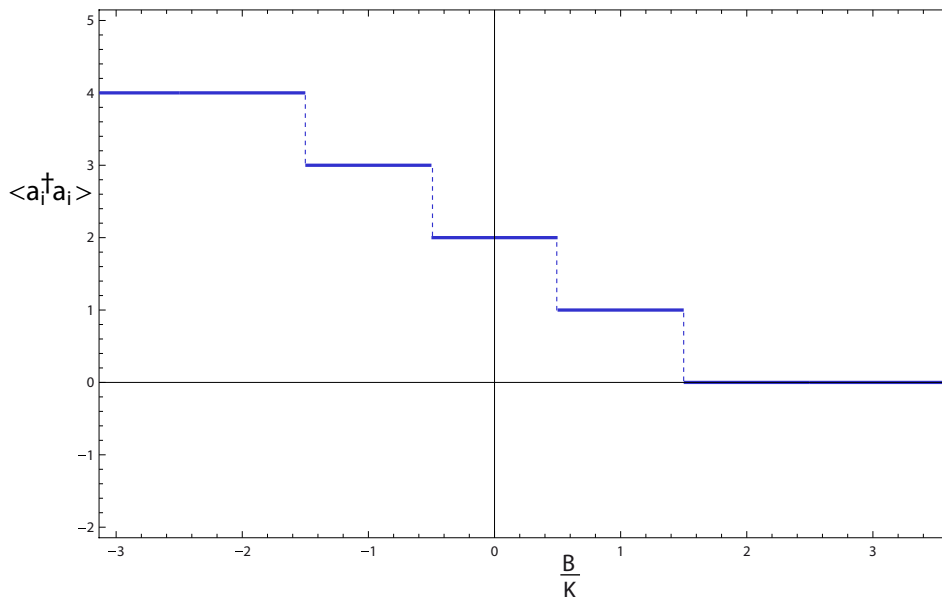In Fig. 6 we plot the results for $S = 2$.

Figure 6: $\langle a_i^\dagger a_i \rangle$ at $T = 0$ for a single spin-2 particle

In this figure, we see that when $\frac{B}{K} > \frac{3}{2}$, $\langle a^\dagger a \rangle = 0$ and so there are no magnons. This is because the magnetic field is strong enough to completely align the spin. Once B drops, the spin will not be forced so strongly to align with the magnetic field, so the spin gains some freedom and can lower its easy-plane anisotropy energy. This freedom means the spin angle can vary. Thus,

magnons are created, more so as the magnetic field weakens, up to a maximum of $2S$ per lattice site. We already noted this maximum when we first considered the Holstein-Primakoff transformation.

Let us now calculate $\langle S_z \rangle$ in the case that $T \neq 0$. Once again, we divide eigenvalues by K so that we can plot over the domain of $\frac{B}{K}$. This leaves βK as adjustable parameter in the canonical ensemble average of S_z:

$$\langle S_z \rangle = \frac{1}{Z} \sum_{m_s=-S}^{S} m_s \hbar e^{-\beta(\frac{K}{2}m_s^2 + \frac{B}{K}m_s m_s)} = \frac{1}{Z} \sum_{m_s=-S}^{S} m_s \hbar e^{-\beta K(\frac{1}{2}m_s^2 + \frac{B}{K}m_s)} \ , \tag{23}$$

where $Z = \sum\limits_{m_s=-S}^{S} e^{-\beta K(\frac{1}{2}m_s^2 + \frac{B}{K}m_s)}$.

Then, after using the Holstein-Primakoff transformation again, we can plot $\langle a_i^\dagger a_i \rangle_{T \neq 0}$ for several values of βK. But before we do so, we'll calculate the variance in the amount of magnons per lattice site, $\sigma^2_{\langle a_i^\dagger a_i \rangle} = \langle (a_i^\dagger a_i)^2 \rangle - \langle a_i^\dagger a_i \rangle^2$. To do so we use the Holstein-Primakoff transformation again and work out the squares:

$$\langle (a_i^\dagger a_i)^2 \rangle = \frac{\langle S_z^2 \rangle}{\hbar^2} + 2S\frac{\langle S_z \rangle}{\hbar} + S^2 \ , \quad \text{while} \quad \langle a_i^\dagger a_i \rangle^2 = \frac{\langle S_z \rangle^2}{\hbar^2} + 2S\frac{\langle S_z \rangle}{\hbar} + S^2$$

$$\text{Therefore,} \quad \sigma^2_{\langle a_i^\dagger a_i \rangle} = \frac{\langle S_z^2 \rangle - \langle S_z \rangle^2}{\hbar^2} \ . \tag{24}$$

In Fig. 7 we plot $\langle a_i^\dagger a_i \rangle_{T \neq 0}$ and $\sigma^2_{\langle a_i^\dagger a_i \rangle}$ for several values of βK.

We see that for nonzero temperature, thermal fluctuations are introduced. At low temperatures (so high values of βK) these just peak around the tipping points from x to y magnons. This uncertainty in magnon quantity becomes more widespread as the temperature increases, until it doesn't even reach zero any more in the middle of the magnon plateaus. By then, the discrete ladder of magnon quantity is barely recognizable. Increase the temperature even further and thermal fluctuations are so high that the entire ladder becomes a smooth line, governed by large variance.

3.3 No interactions neglected: variance at $T = 0$

We have seen that for a single spin at zero temperature, varying the magnetic field will create and annihilate magnons in a discrete ladder. However, a single spin does not consider magnon propagation between sites, so we now calculate the variance of magnon quantity per lattice site at zero temperature $\sigma^2_{\langle a_i^\dagger a_i \rangle} = \langle (a_i^\dagger a_i)^2 \rangle - \langle a_i^\dagger a_i \rangle^2$ without neglecting interactions between sites.

Suppose our system consists of N (bosonic and identical) magnons in the groundstate, which we denote by $|\Psi_{T=0}^N\rangle$. Next we define the vacuum state of our system with zero magnons as $|0\rangle$, where $\langle 0|0\rangle = 1$. Our system groundstate is formed by creating N magnons with wave vector $\vec{0}$ in this vacuum state, so

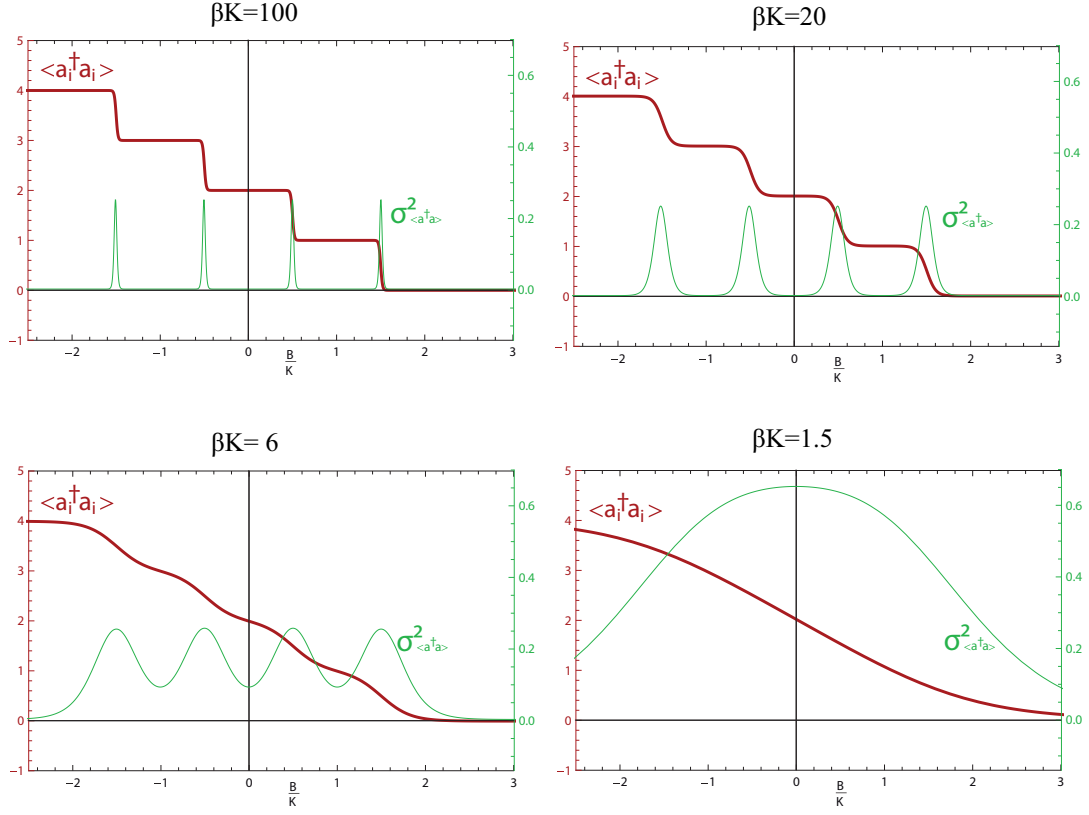$$|\Psi_{T=0}^N\rangle = A(a_{\vec{0}}^\dagger)^N |0\rangle \ , \tag{25}$$

Figure 7: $\langle a_i^\dagger a_i \rangle$ and $\sigma^2_{\langle a_i^\dagger a_i \rangle}$ at $T \neq 0$ for a single spin-2 particle

where A is a normalization factor to be determined. To normalize this expression we use the relations known for bosonic creation and annihilation operators:

$$a_{\vec{k}}^\dagger |n\rangle = \sqrt{n+1}|n+1\rangle \quad , \quad a_{\vec{k}}|n-1\rangle = \sqrt{n}|n\rangle \ , \tag{26}$$

where $|n\rangle$ denotes the state with n magnons in our system, with $\langle n|n\rangle = 1$. Now, the groundstate should also obey $\langle \Psi_{T=0}^N | \Psi_{T=0}^N \rangle = 1$. We can use the above relations to normalize this state:

$$A^2 \langle 0|(a_{\vec{0}})^N (a_{\vec{0}}^\dagger)^N |0\rangle = (1) \times A^2 \langle 1|(a_{\vec{0}})^{N-1} (a_{\vec{0}}^\dagger)^{N-1}|1\rangle$$
$$= (2) \times (1) \times A^2 \langle 2|(a_{\vec{0}})^{N-2} (a_{\vec{0}}^\dagger)^{N-2}|2\rangle = N! \times A\langle N|N\rangle = 1 \ . \tag{27}$$

This leads us to the expression for our groundstate:

$$|\Psi_{T=0}^N\rangle = \frac{1}{\sqrt{N!}}(a_{\vec{0}}^\dagger)^N |0\rangle \ . \tag{28}$$

Before we continue to calculate the average amount of particles per lattice site, $\langle a_i^\dagger a_i \rangle$, we derive the commutation relation $[a_{\vec{k}}, (a_{\vec{0}}^\dagger)^N]$, which will be useful in later calculations. First we use the known relation $[a_{\vec{k}}, a_{\vec{0}}^\dagger] = \delta_{\vec{k},\vec{0}}$. Using

Leibniz' rule for commutation relations ($[A, BC] = B[A, C] + [A, B]C$), we find that $[a_{\vec{k}}, (a_{\vec{0}}^\dagger)^2] = 2\delta_{\vec{k},\vec{0}}a_{\vec{0}}^\dagger$. After a few iterations we come to the conclusion that

$$[a_{\vec{k}}, (a_{\vec{0}}^\dagger)^N] = N\delta_{\vec{k},\vec{0}}(a_{\vec{0}}^\dagger)^{N-1} \ . \tag{29}$$

And finally, since our groundstate is given in momentum space, we make use of the Fourier transformation $a_j^\dagger = \frac{1}{\sqrt{N}} \sum_{\vec{k}} e^{-i\vec{k}\cdot\vec{x}_j} a_{\vec{k}}^\dagger$. Now we calculate the average amount of magnons per lattice site:

$$\langle a_j^\dagger a_j \rangle = \frac{1}{N_s} \sum_{\vec{k},\vec{k}'} e^{-i\vec{k}\cdot\vec{x}_j} e^{i\vec{k}'\cdot\vec{x}_j} \times \frac{1}{N!} \langle 0|(a_{\vec{0}}^\dagger)^N a_{\vec{k}} a_{\vec{k}'}^\dagger (a_{\vec{0}}^\dagger)^N|0\rangle \ . \tag{30}$$

Here the expectation value vanishes unless $\vec{k} = \vec{k}'$, because if you remove a particle of state $\vec{k}'$ from the groundstate, and put it back in state $\vec{k}$, the new state will be orthogonal to the groundstate. Thus we are just left with $\sum_{\vec{k}} \frac{1}{N_s} \langle \Psi_{T=0}^N | a_{\vec{k}'}^\dagger a_{\vec{k}} | \Psi_{T=0}^N \rangle = \frac{N}{N_s}$, because this expression basically counts the amount of magnons in the groundstate in our lattice with any wave vector $\vec{k}$, which are exactly all the magnons we defined in our lattice.

In a similar fashion we start to calculate

$$\langle (a_j^\dagger a_j)^2 \rangle = \frac{1}{N_s^2 N!} \sum_{\vec{k},\vec{k}',\vec{k}'',\vec{k}'''} e^{-i\vec{k}\cdot\vec{x}_j} e^{i\vec{k}'\cdot\vec{x}_j} e^{i\vec{k}''\cdot\vec{x}_j} e^{i\vec{k}'''\cdot\vec{x}_j} * \frac{1}{N!} \langle 0|(a_{\vec{0}}^\dagger)^N a_{\vec{k}} a_{\vec{k}'}^\dagger a_{\vec{k}''}^\dagger a_{\vec{k}'''} (a_{\vec{0}}^\dagger)^N|0\rangle \ . \tag{31}$$

We then use the commutation relation we derived above to write $a_{\vec{k}'''}(a_{\vec{0}}^\dagger)^N|0\rangle = N\delta_{\vec{k},\vec{0}}(a_{\vec{0}}^\dagger)^{N-1}|0\rangle + (a_{\vec{0}}^\dagger)^N a_{\vec{k}'''}|0\rangle$ and similarly for the left side of the expectation value. We note that the second term is equal to zero because the annihilation operator acting on the empty vacuum state leaves us with nothing. Analogous to the above line of thought the expectation value vanishes again unless $\vec{k}' = \vec{k}''$. We are left with the expression

$$\frac{N^2}{N_s^2 N!} \sum_{\vec{k}'} \langle 0|(a_{\vec{0}}^\dagger)^{N-1} a_{\vec{k}'} a_{\vec{k}'}^\dagger (a_{\vec{0}}^\dagger)^{N-1}|0\rangle$$

$$= \frac{N^2}{N_s^2 N!} \sum_{\vec{k}} \langle 0|(a_{\vec{0}}^\dagger)^{N-1}(1 + a_{\vec{k}}^\dagger a_{\vec{k}})(a_{\vec{0}}^\dagger)^{N-1}|0\rangle$$

$$= \frac{N^2}{N_s^2 N} \sum_{\vec{k}} \langle \Psi_{T=0}^{N-1}|(1 + a_{\vec{k}}^\dagger a_{\vec{k}})|\Psi_{T=0}^{N-1}\rangle \tag{32}$$

$$= \frac{N(N-1)}{N_s^2} + \sum_{\vec{k}} \frac{N}{N_s^2} \ .$$

Thus we find that the variance $\sigma^2_{\langle a_i^\dagger a_i \rangle} = \langle (a_i^\dagger a_i)^2 \rangle - \langle a_i^\dagger a_i \rangle^2 = -\frac{N}{N_s^2} + \sum_{\vec{k}} \frac{N}{N_s^2}$.

This is evidently a quantum fluctuation at zero temperature. Going back to the $T = 0$ plot when considering a single spin (so $J = 0$), we found a discrete ladder with no variance across the domain. We therefore conclude that this was also a crude approximation that neglects certain properties that may be important for the phase diagram which we want to obtain.

4 Mott insulating regions: a mean-field approach

A different approach must be used to obtain the transitions to the Mott insulating regions of our system, which are a lot more detailed than we can expect to accurately show with the evidently crude approximations used so far. A way to obtain these transitions was proposed by van Oosten et al.[11] They started with the observation shown by Jaksch et al.[14] that a system of bosonic atoms trapped in an optical lattice could be described by the Bose-Hubbard Hamiltonian. They then used several approaches to construct a phase diagram, of which a mean-field approach yielded results. With this approach, they were able to predict the Mott-insulating boundaries of the atoms in their system. Since our magnons obey bosonic statistics, we may be able to show our transitions with analogous calculations.

Let us try a mean-field approach for our system then, to see which results its yields. We first use the most basic approach imaginable: $a_i \implies \langle a_i \rangle$, thus transforming every creation and annihilation operator to its expectation value. This expectation value then, is the square root of the expected amount of magnons per lattice site, an order parameter in our system which we call ϕ. Rewriting our Hamiltonian (Eq. (12)) in terms of ϕ we obtain the free energy:

$$E = N_s(\frac{K}{2}(1 - 2S) + B)\phi^2 + \frac{KN_s}{2}\phi^4 \ . \tag{33}$$

Minimizing the free energy with respect to the order parameter gives us an expression for the order parameter: $\phi = \sqrt{\langle n_i \rangle} = \sqrt{S - \frac{1}{2} - \frac{B}{K}}$. We plot the results in Fig. 8.
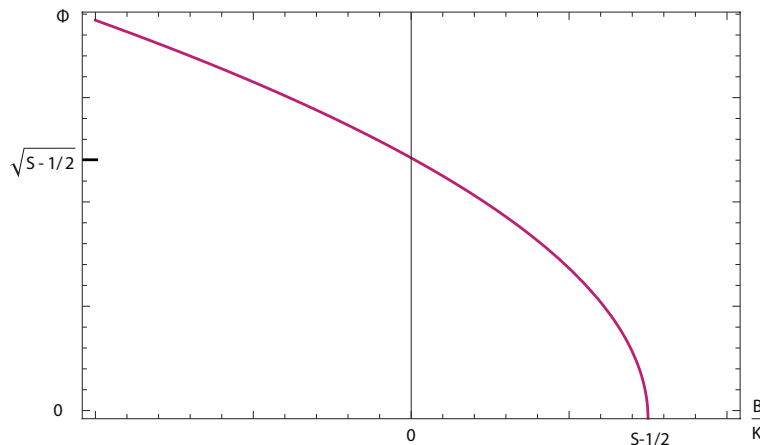

Figure 8: Order parameter ϕ that minimizes the free energy

We see that the order parameter reaches zero when $B/K = S - 1/2$, a familiar quantity by now. This backs up our previously found results that this is indeed a critical point at which a phase transition occurs to the superfluid phase.

In their paper, van Oosten et al. used a more advanced Mean-field approach. Their method was based on a mean-field order parameter they introduced that made it possible to describe their system by an uncoupled Hamiltonian. They

then used second-order pertubation theory to find an expression for the boundary between the superfluid and Mott insulator phases. Since their system is mathematically very similar to ours, we compare our system to theirs, so that we can use their theoretical results to construct a phase diagram for our lattice with magnons. Their system is described by the Hamiltonian

$$H = -t \sum_{\langle i,j \rangle} a_i^\dagger a_j + \frac{U}{2} \sum_i a_i^\dagger a_i^\dagger a_i a_i - \mu \sum_i a_i^\dagger a_i . \qquad (34)$$

Comparing this with our Hamiltonian (Eq.(8)) we find that it is identical, after we throw away the fourth order term $-\frac{J}{2} \sum_{\langle i,j \rangle} a_i^\dagger a_j^\dagger a_i a_j$. We then define their parameters as $t = JS$, $U = K$ and $\mu = -(\frac{K}{2}(1-2S) + B + \frac{JSz}{2})$, so that our Hamiltonians are identical.

After extensive calculations van Oosten et $al.$ find their expression for the boundary between the superfluid and insulator phases that is exact within their mean-field approach:

$$\bar{\mu}_\pm = \frac{1}{2}[\bar{U}(2\langle a_i^\dagger a_i \rangle - 1) - 1] \pm \frac{1}{2}\sqrt{\bar{U}^2 - 2\bar{U}(2\langle a_i^\dagger a_i \rangle + 1) + 1} , \qquad (35)$$

where the subscript $\pm$ denotes the upper and lower halves of the Mott insulating regions of phase space. Further $\bar{U} = U/zt$, $\bar{\mu} = \mu/zt$, and $\langle a_i^\dagger a_i \rangle$ is the amount of magnons per lattice site.

Since we made the comparison of their parameters with ours, we can directly substitute these in this expression for $\bar{\mu}$. But since we also have $\bar{\mu} = \mu/zt = -(\frac{K}{2}(1-2S) + B + \frac{JSz}{2}) = -(\frac{\bar{K}}{2}(1-2S) + \bar{B}\bar{K} + \frac{1}{2})$, we can equate these expressions and solve it for $\frac{J}{K}$, which gives a boundary between our magnon superfluid and insulating phases. We plot this boundary for $\langle a_i^\dagger a_i \rangle = 1, 2, 3, 4$ in Fig. 9.
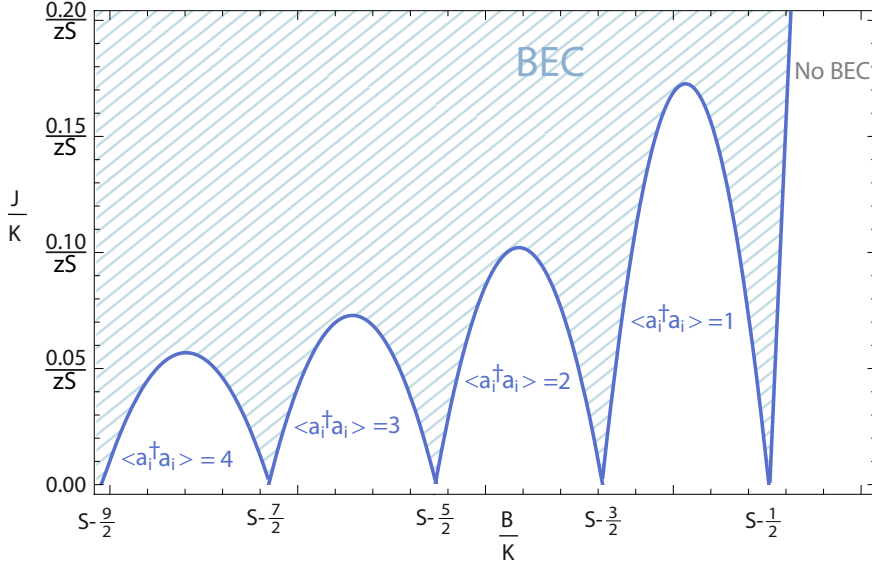

Figure 9: Mott insulating regions after mean-field approach of van Oosten et $al.$

18

Here, z is again the amount of nearest-neighbour lattice sites. We see these bulges appear within the blue-striped region of BEC, which is fairly consistent with the previously calculated threshold $\frac{B}{K} = S - \frac{1}{2}$ (there independent T and J) when we neglected interactions. Within these bulges BEC is broken and the system resides in the Mott insulator phase. The bulges appear only for an integer value of $\langle a_i^\dagger a_i \rangle$, which means that all lattice sites contain the same integer amount of magnons. This is in accordance with the theory we gave of the Mott insulating phase: with the same amount of magnons on each site, they will not hop to other sites (see Fig. 3), and thus the freedom in spin angle remains unaligned and BEC is broken.

We also see that the insulating regions only appear within a very limited range of J/K, that grows even smaller when we work with higher spins or higher dimensions. Further we note that the bulges grow even smaller as $\langle a_i^\dagger a_i \rangle$ increases. Although $\langle a_i^\dagger a_i \rangle$ seems unrestricted, we had to keep in mind that any state with $\langle a_i^\dagger a_i \rangle$ larger than $2S$ is unphysical (as discussed before). Therefore the Mott insulating region bulges will in fact stop after $\langle a_i^\dagger a_i \rangle = 2S$.

In response to an earlier version of this diagram, Stoof (co-author of Ref. [11]) made the suggestion that the region labeled as "No BEC" could be viewed as the Mott insulating region for $\langle a_i^\dagger a_i \rangle = 0$, so for zero magnons in our system. Calculations were made and accordingly the BEC boundary was updated to match this useful observation.

Thus we have created a phase diagram showing the superfluid and Mott insulating phases of magnons in a ferromagnetic lattice. In the next chapter we check whether the results we just found are trustworthy.

5 Comparing the Spin- and Bose-Hubbard Hamiltonian

To map the phase transitions to a Mott insulating state of magnons in our system we used the mean-field approximations of the Bose-Hubbard Hamiltonian. But remember, to obtain the Bose-Hubbard Hamiltonian form the Spin-Hamiltonian, we used a Holstein-Primakoff transformation followed by a truncated Taylor expansion in powers of $1/S$. We expect that because of this expansion, we will find some differences between the results predicted by the Spin- and Bose-Hubbard Hamiltonian, especially when S is small. We want to investigate just how accurate will the predictions made by the Bose-Hubbard Hamiltonian are for our system of magnons, so that we can argue how valid the phase diagram we just obtained is. To do so, we compare the expectation value of the total amount of magnons $\langle a^\dagger a \rangle$ in a crystal with 2 lattice sites, and evaluate this expectation value both from the exact spin-Hamiltonian and the Bose-Hubbard Hamiltonian.

5.1 Expectation values for $S = 1$ using the spin-Hamiltonian

Our spin-Hamiltonian (Eq. (1)), written out for two lattice sites in one dimension (of which the last is connected to the first one again), reads

$$H = -\frac{J}{2\hbar^2}\vec{S_1} \cdot \vec{S_2} + \frac{K}{2\hbar^2}((S_1^z)^2 + (S_2^z)^2) + \frac{B}{\hbar}(S_1^z + S_2^z) . \qquad (36)$$

This Hamiltonian acts in the direct product space $T_{S_1} \otimes T_{S_2}$, spanned by the direct product states $|m_{s,1}\rangle \otimes |m_{s,2}\rangle$, where $m_{s,i}$ ranges from $-S_i$ to S_i. We first consider two spin-1 particles, so that a basis of our space is formed by the nine states

$$
\begin{array}{ccc}
|1\rangle \otimes |1\rangle & |1\rangle \otimes |0\rangle & |1\rangle \otimes |\text{-}1\rangle \\
|0\rangle \otimes |1\rangle & |0\rangle \otimes |0\rangle & |0\rangle \otimes |\text{-}1\rangle \\
|\text{-}1\rangle \otimes |1\rangle & |\text{-}1\rangle \otimes |0\rangle & |\text{-}1\rangle \otimes |\text{-}1\rangle \ .
\end{array}
\tag{37}
$$

To find a matrix representation for our Hamiltonian in this basis, we use the matrix-representations of the spin operators for spin-1:

$$
\sigma_x = \frac{\hbar}{\sqrt{2}} \begin{pmatrix} 0 & 1 & 0 \\ 1 & 0 & 1 \\ 0 & 1 & 0 \end{pmatrix}, \ \sigma_y = \frac{i\hbar}{\sqrt{2}} \begin{pmatrix} 0 & \text{-i} & 0 \\ i & 0 & \text{-i} \\ 0 & i & 0 \end{pmatrix}, \ \sigma_z = \hbar \begin{pmatrix} 1 & 0 & 0 \\ 0 & 0 & 0 \\ 0 & 0 & \text{-1} \end{pmatrix} \ ,
$$

The spin operators in this Hilbert space are now obtained by taking, for example, $S_1^z = \sigma_z \otimes \mathbb{I}$, so that S_1^z acts upon the first lattice site as usual, while trivially acting on the second one. Similarly we use $S_2^z = \mathbb{I} \otimes \sigma_z$, and $\vec{S_1} \cdot \vec{S_2} = \sigma_{x_1} \otimes \sigma_{x_2} + \sigma_{y_1} \otimes \sigma_{y_2} + \sigma_{z_1} \otimes \sigma_{z_2}$, where $\mathbb{I}$ is the 3x3 identity matrix. We then calculate the 9x9 matrix representation of our Hamiltonian. To make the calculations less complicated, we divide this Hamiltonian by K, so that it is only dependent on $\frac{J}{K}$ and $\frac{B}{K}$. We diagonalize this matrix to find its eigenvalues and corresponding vectors. After normalization these 9-component vectors represent the eigenstates of our Hamiltonian and are dependent on $\frac{J}{K}$. We can now continue to calculate some expectation values.

Let's start with our system in the groundstate, for $J = 0$. Since the two particles are then uncoupled, we expect the same results as we calculated before for a single-spin, only now multiplied by 2. We select the groundstates of our diagonalized Hamiltonian, which are again dependent on $\frac{B}{K}$. We can then calculate $\langle S_{tot,z} \rangle_{T=0} = \langle S_{1,z} + S_{2,z} \rangle_{T=0} = \langle \Psi_{gs} | S_{1,z} + S_{2,z} | \Psi_{gs} \rangle$, and use the Holstein-Primakoff transformation to translate the results in terms of magnons. We plot the results in Fig. 10.
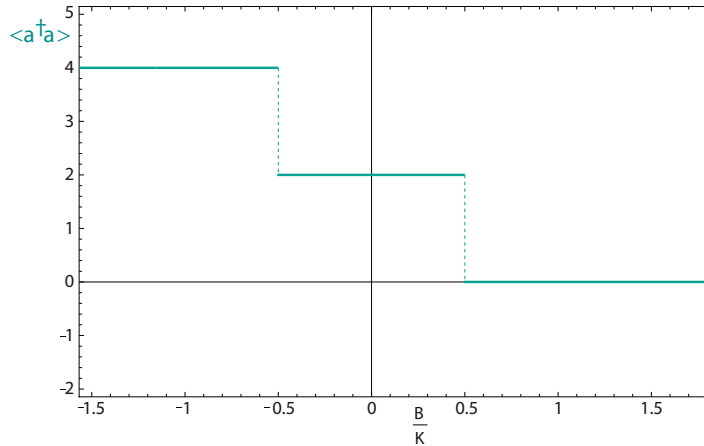

Figure 10: $\langle (a^\dagger a)_{tot} \rangle$ at $T = 0$ and $J = 0$ for two spin-1 particles

We see that this is exactly what we anticipated. The two lattice sites are un-coupled and therefore magnons are created at both sites on the exact thresholds as we calculated for single spins.

Next we calculate the expectation value $\langle S_z \rangle$ when $T \neq 0$ and $J \neq 0$. We do this (as before) by taking the canonical ensemble average:

$$\langle S_{tot,z} \rangle = \langle S_{1,z} + S_{2,z} \rangle = \frac{\sum_n \langle \Psi_n | S_{1,z} + S_{2,z} | \Psi_n \rangle e^{-\beta \langle \Psi_n | H | \Psi_n \rangle}}{\sum_n e^{-\beta \langle \Psi_n | H | \Psi_n \rangle}} \quad . \tag{38}$$

In a similar fashion we calculate $\langle S_{tot,z}^2 \rangle$ and the variance of $S_{tot,z}$. After using the Holstein-Primakoff transformation we plot the results for $\beta K = 100$ (since we are interested in the behaviour at low temperatures, where the phase transistions occur) and several values of $\frac{J}{K}$ in Fig. 11.
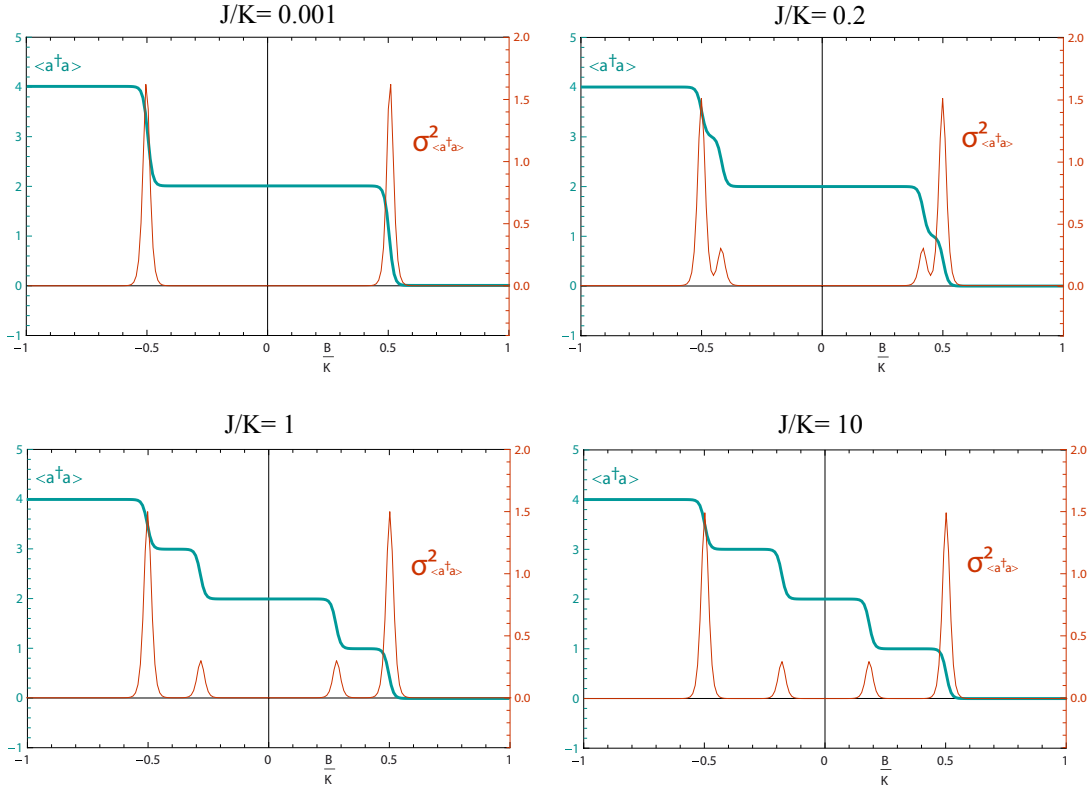

Figure 11: $\langle (a^\dagger a)_{tot} \rangle$ and $\sigma^2_{\langle (a^\dagger a)_{tot} \rangle}$ for $\beta K = 100$ for two spin-1 particles

We see that when J/K is small, the system behaves like the sum of two uncoupled particles which we calculated before. This was to be expected, since J is the term that controls interactions between the sites. As J/K increases, we see that when 1 magnon is created in the lattice, the threshold for the second magnon to be created is shifted, due to interaction energies between sites. When J/K is large, these thresholds even out so that all steps in the ladder of magnon creation and annihilation are of the same size in their domain of B/K.

5.2 Expectation values for $S = 1$ using the Bose-Hubbard Hamiltonian

Now we calculate the same expectation values using the Bose-Hubbard Hamiltonian, so that we can compare its results. To do so, we have to write out Eq. (12) for two lattice sites, again in 1 dimension and where the second site is connected to the first one. To get rid of the sums over pairs we write $\sum_{\langle i,j \rangle} a_i^\dagger a_j = \frac{1}{2} \sum_i a_i^\dagger (a_{i+1} + a_{i-1})$, and similarly for the fourth order term in J. We obtain the Hamiltonian:

$$
\begin{aligned}
H = &-J[S(a_1^\dagger a_2 + a_2^\dagger a_1) + \frac{1}{2}(a_1^\dagger a_2^\dagger a_1 a_2 + a_2^\dagger a_1^\dagger a_2 a_1)] \\
&+ [\frac{K}{2}(1 - 2S) + B + JS](a_1^\dagger a_1 + a_2^\dagger a_2) + \frac{K}{2}(a_1^\dagger a_1^\dagger a_1 a_1 + a_2^\dagger a_2^\dagger a_2 a_2) .
\end{aligned}
\tag{39}
$$

The Hilbert space on which this Hamiltonian acts is spanned by the states $|n_1\rangle \otimes |n_2\rangle$, where n_1 and n_2 represent the amount of magnons on lattice site 1 and 2, respectively. A matrix representation of $a^\dagger$ and a acting on a single site is then:

$$
a^\dagger = \begin{pmatrix} 0 & 0 & 0 & \dots & 0 & \dots \\ \sqrt{1} & 0 & 0 & \dots & 0 & \dots \\ 0 & \sqrt{2} & 0 & \dots & 0 & \dots \\ \vdots & \vdots & \vdots & \ddots & 0 & \dots \\ 0 & 0 & 0 & \sqrt{n} & 0 & \dots \\ \vdots & \vdots & \vdots & \vdots & \ddots & \ddots \end{pmatrix} , \ a = \begin{pmatrix} 0 & \sqrt{1} & 0 & \dots & 0 & \dots \\ 0 & 0 & \sqrt{2} & \dots & 0 & \dots \\ 0 & 0 & 0 & \dots & 0 & \dots \\ \vdots & \vdots & \vdots & \ddots & \sqrt{n} & \dots \\ 0 & 0 & 0 & 0 & 0 & \ddots \\ \vdots & \vdots & \vdots & \vdots & \vdots & \ddots \end{pmatrix} ,
\tag{40}
$$

where n is the maximum amount of magnons on that lattice site.

Note that n seems to be unrestriced, i.e. there can be an arbitrary amount of magnons on each lattice site. This is a result of the truncated Taylor expansion from the Holstein-Primakoff transformation we used to obtain the Bose-Hubbard Hamiltonian. As mentioned, we should keep in mind that before we used that approximation, it could be seen that any state with more than $2S$ magnons one one site is unphysical. We have an opportunity here to research what the Bose-Hubbard Hamiltonian predicts when we make caluations with these unphysical states, but for now we will cut off the matrix representations of $a^\dagger$ and a so that no more than $2S$ magnons can be created per lattice site.

We then take $S = 1$ so that we can construct the operators of our Hamiltonian by taking $a_1^\dagger = a^\dagger \otimes \mathbb{I}_3$ and $a_2^\dagger = \mathbb{I}_3 \otimes a^\dagger$ and similar for a_1 and a_2. With these, we then find a 9x9 matrix representation of the Bose-Hubbard Hamiltonian, which we divide by K again. After diagonalizing this matrix we find that the eigenvectors are this time dependent on both J/K and B/K.

The Bose-Hubbard Hamiltonian as used in the calculations by van Oosten *et al.* lacked the fourth order J-term, since it would make analytical elaboration impossible. Since we used their calculations to map the transition from insulator to superfluid phase of our system, we'd like to see the difference between the results of the Bose-Hubbard Hamiltonian when this fourth order term is excluded and included.

In the usual way we calculate the thermal average $\langle(a^\dagger a)_{tot}\rangle$. When we take $J = 0$, the results are exactly the same as for the Spin-Hamiltonian. This is hardly surprising, since the Taylor expansion we used was only included in the coupled terms. When we take $J \neq 0$, the results begin to deviate rapidly. In Fig. 12 we plot the results for $\beta K = 100$ of the Bose-Hubbard Hamiltonian including the fourth order term (blue) and without the fourth order term (red), and compare them with the previous results from the Spin-Hamiltonian (yellow).
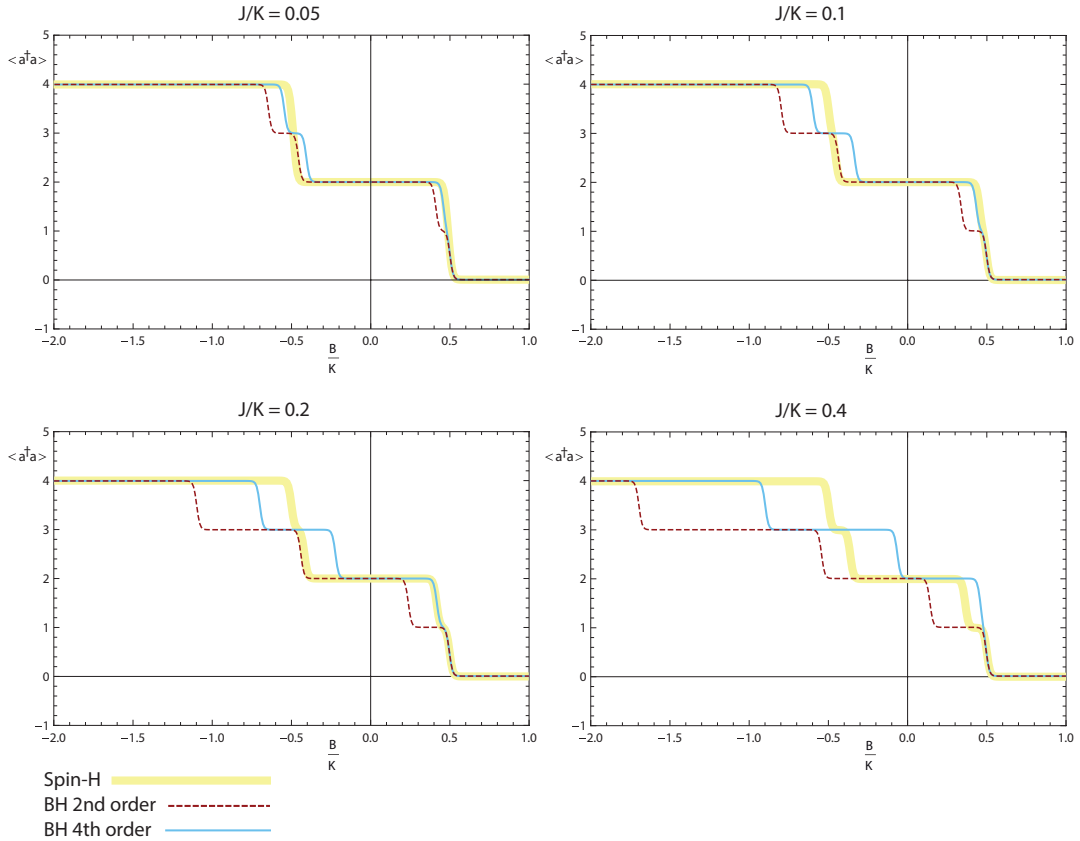

Figure 12: $\langle(a^\dagger a)\rangle_{tot}$ at $\beta K = 100$ for the Spin-Hamiltonian and Bose-Hubbard 2nd and 4th-order Hamiltonian for $S = 1$

As we can see, even for very small values of J/K the second order Bose-Hubbard Hamiltonian differs from the Spin-Hamiltonian. It is accurate for the first magnon created, but then the differences become ever larger for every second magnon that's created. The difference only magnifies as J/K rises, and is already huge by the time that $J/K = 0.4$.

The fourth order Bose-Hubbard Hamiltonian fares slightly better. In a greater range of J/K it remains accurate in predicting the threshold for the first two magnons created in our lattice. The third and fourth magnons of our system are less accurate, but the overall deviations from the Spin-Hamiltonian are still about half of those observed from the second order Bose-Hubbard Hamiltonian.

As discussed, we expected differences because to obtain the Bose-Hubbard

Hamiltonian we expanded an expression around zero in powers of $1/S$. Since we now took $S = 1$, this whole expansion is not very well legitimated. Were we to consider our system for higher spin, however, we would expect to find more accurate results.

5.3 Expectation values for $S = 2$

Therefore, we now calculate the same expectation values for $S = 2$. This means that for the Spin-Hamiltonian, we use the spin-2 matrices instead of those for spin-1, and for the Bose-Hubbard Hamiltonian, we cut off the infinite matrix representation for $a^\dagger$ and a to permit a maximum of $2S = 4$ magnons per lattice site, instead of 2. Calculations are analogous to those for spin-1, only now we obtain a 25x25 matrix representation for both the Spin- and Bose-Hubbard Hamiltonians, which considerably lengthens the time needed for the calculations to be completed. The results are plotted in Fig. 13.
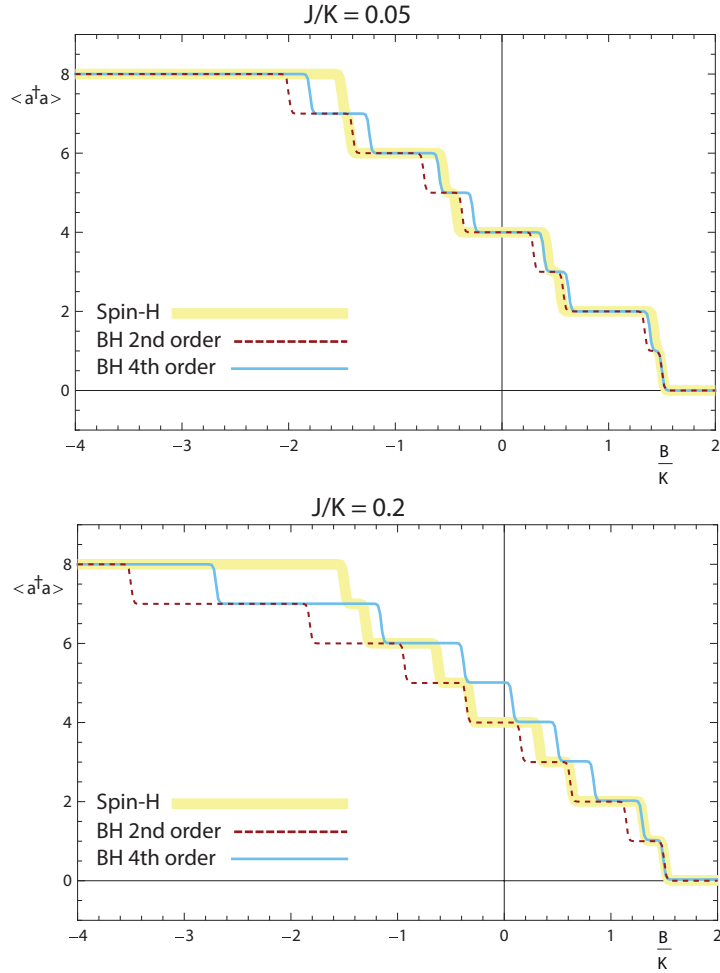

Figure 13: $\langle(a^\dagger a)\rangle_{tot}$ at $\beta K = 100$ for the Spin-Hamiltonian and Bose-Hubbard 2nd and 4th-order Hamiltonian for $S = 2$

The results are similar to what we found for $S = 1$. As soon as $J \neq 0$, the Bose-Hubbard Hamiltonian deviates from the Spin-Hamiltonian. When J/K is small enough, the fourth-order Bose-Hubbard Hamiltonian is fairly accurate in predicting the threshold for creation of the first 4 magnons in our lattice, but this accuracy quickly deteriorates; when $J/K = 0.2$, only the first 2 magnons are predicted nicely and above that the fourth order Bose-Hubbard Hamiltonian barely gives better results than the second order. Still, in all, the ladders as predicted by all Hamiltonians are not completely dissimilar. It is imaginable that for higher spin the approximation will slowly improve, but a comparison of the results from spin-1 and spin-2 is inconclusive in this respect.

5.4   Expectation values for $S = 6$

We therefore take a large step to spin-6. As the matrix representations of the spin operators S_x, S_y, S_z for $S = 6$ are uncommon to find in literature, we use the known eigenvalues of the operators to construct these three 13x13 matrices ourselves to calculate the spin-Hamiltonian. For the Bose-Hubbard Hamiltonian, we cut off the matrices for $a^\dagger$ and a to permit a maximum of $2S = 12$ magnons per lattice site. Both Hamiltonians are now 169x169 matrices. To calculate the wanted expectation values (again, completely analogous to the methods above) for these large matrices, optimized programming and a lot of patience are needed. We therefore only compute $\langle (a^\dagger a)_{tot} \rangle$ for $\beta K = 100$ and $J/K = 0.1$ for the spin- and 2nd-order Bose-Hubbard Hamiltonian, and plot the results in Fig. 14.
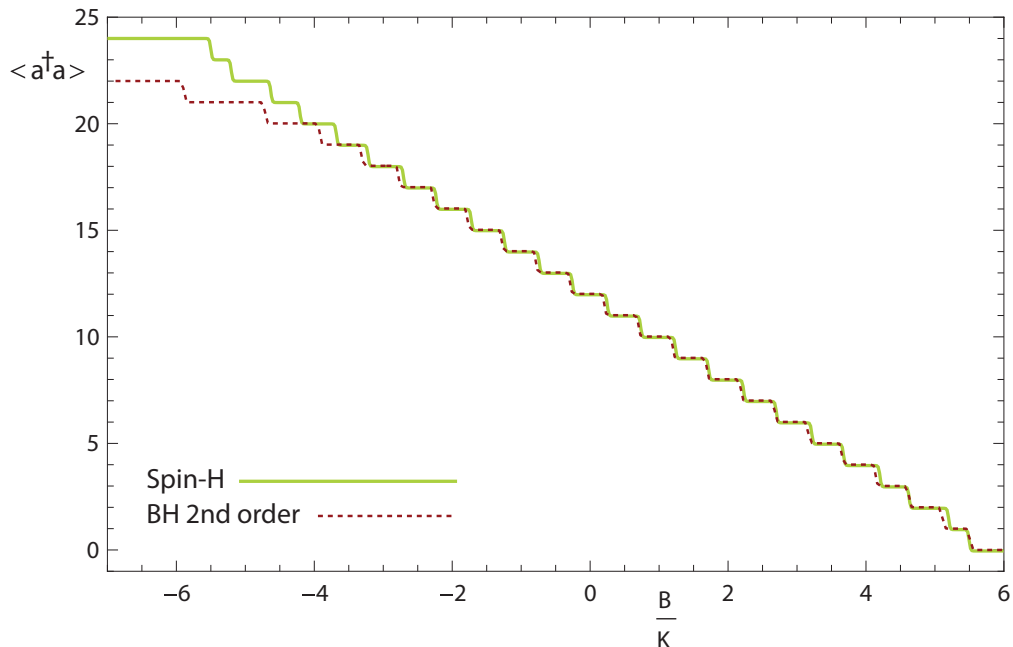

Figure 14: $\langle (a^\dagger a) \rangle_{tot}$ at $\beta K = 100$ and $J/K = 0.1$ for the Spin-Hamiltonian and Bose-Hubbard 2nd-order Hamiltonian for $S = 6$

We immediately see that the results are much more accurate than before.

A few minor differences can be discerned in the first magnons when comparing the second-order Bose Hubbard Hamiltonian to the spin-Hamiltonian, but they only grow larger after about 18 magnons (out of the maximum of 24 that can be created in this system). We now have enough results to make a reasonable conclusion.

6 Conclusion

A phase diagram of the superfluid and Mott insulating regions of magnons in a ferromagnetic lattice has been obtained (see Fig. 9). In order to use the calculations done by van Oosten *et al.* to map the Mott insulating regions of this system, we were obliged to describe our lattice by a form of the Bose-Hubbard Hamiltonian. This could be done by using a Taylor expansion and subsequently neglecting a fourth order term we obtained. We compared the expectation value of the amount of magnons in a two-site, one-dimensional lattice, using both this approximated Hamiltonian and the original spin-Hamiltonian.

When taking $S = 6$, we found that the first three-quarter of the magnons in our two-site lattice were accurately predicted by the approximated Bose-Hubbard Hamiltonian. We can therefore conclude that this Hamiltonian is fairly trustworthy in showing the first three-quarter of the bulges of Mott insulating regions in our phase diagram. There, it predicts that the first bulge always stays below $\frac{J}{K} = \frac{0.2}{zS}$, which is much smaller than the $J/K = 0.1$ at which the deviations of the Bose-Hubbard Hamiltonian were tested. Successive regions of Mott insulating phases only appear for increasing smaller values of J/K, and we expect this tendency to continue when the regions seem less accurately predicted (after about three-quarter of the regions). For the small values of J/K that those regions then exist, the differences between the Bose-Hubbard- and the spin-Hamiltonian have almost vanished (i.e. they are not nearly as large as tested in Fig. 14). We therefore argue that for $S = 6$ even more than three-quarter of these regions are fairly reliably shown in our phase diagram. This is especially true when working in higher dimensions, since then accuracy everywhere is enhanced, because the insulating regions exist for even smaller values of J/K than discussed above. When considering a lattice of particles of higher spin, results will also become increasingly accurate, both because the used Taylor expansion is better legitimated and because the Mott regions will appear for lower values of J/K.

When the particles in the lattice are of a lower spin, more care must be taken. Large deviations of the expectation values from the Bose-Hubbard Hamiltonian are seen even at small values of J/K, so we should be more suspicious of the results it yields for the Mott insulating regions at these lower spins. For $S = 2$ and $S = 1$ the Bose-Hubbard Hamiltonian is only accurate when describing the first magnon in a two-site lattice. But we need at least one magnon on both sites in order to be able to reach the first Mott insulating state containing magnons. The second magnon in our two-site example lattice however, is not very accurately predicted by the Bose-Hubbard Hamiltonian, so the phase diagram we obtained cannot be trusted into detail for low spins. This problem could be partially solved by including the fourth-order term in the Bose-Hubbard Hamiltonian which we neglected from Eq. (34) onward. This fourth-order Hamiltonian stays reasonably accurate in describing the first two magnons in our lattice, where

it could transit to the first Mott insulating region. One could then expect a fairly accurately predicted first Mott region for these low spins, especially when working in more than one dimension. This would mean however, that a different approach than used in this thesis should be taken to construct a phase diagram, since our method was based on that of van Oosten *et al.*, where analytical calculations would be impossible when including the relevant fourth-order term.

Further we found a transition of our magnons to a superfluid state when B/K dropped below the threshold of $S - 1/2$. To reach this result, we once again used the second-order Bose-Hubbard Hamiltonian, where now even the fourth order in the K-term was thrown away, thus neglecting on-site magnon-magnon interactions. As discussed in Ref. [13], we know that this boundary is actually not independent of temperature when these interactions are included. At temperatures close to zero our superfluid transition is a reasonable approximation, but some work is still left to be done to obtain an accurate phase diagram showing this transition at higher temperatures.

Other future work includes investigating the accuracy of the predicted transitions for more than two lattice sites and in higher dimensions. Such a many-body problem could be solved numerically using the Gutzwiller ansatz (a factorizable wavefunction), which works well in three dimensions or more.

As for experimental possibilities, Momoi *et al.* [15] have shown that Mott insulating states correspond with plateaus in the magnetization when varying the magnetic field, whereas it is gapless for a superfluid state. Since the magnetic field is an easily adjustable parameter, this link could be exploited to experimentally observe the transitions from a superfluid to a Mott insulating phase as predicted in this thesis.

7 Acknowledgements

8 References

[1] G. Jaeger. "The Ehrenfest Classification of Phase Transitions: Introduction and Evolution" *Archive for History of Exact Sciences* **53**, 51-81 (1998)

[2] J.F. Allen and A.D. Misener. "Flow of liquid Helium II". *Nature* **141**, 75 (1938).

[3] P. Kapitza. "Viscosity of liquid Helium below the 1-point". *Nature* **141**, 74-75 (1938).

[4] A. Einstein. *Sitzungsberichte der Preussischen Akademie der Wissenschaften* **261**, (1924).

[5] M.H. Anderson, J.R. Enscher, M.R. Matthews, C.E. Wieman and E.A. Cornell. "Observation of Bose-Einstein Condensation in a Dilute Atomic Vapor". *Science* **269**, 198-201 (1995).

[6] S.O. Demokritov, V.E. Demidov, O. Dzyapko, G.A. Melkov, A.A. Serga, B. Hillebrands and A.N. Slavin. "Bose-Einstein condensation of quasi-equilibrium magnons at room temperature under pumping". *Nature* **443**, 430 (2006).

[7] N.F. Mott and R. Peierls. "Discussion of the paper by de Boer and Verwey". *Proceedings of the Physical Society* **49**, 72 (1937).

[8] J.H. de Boer and E.J.W. Verwey "Semi-conductors with partially and completely filled 3d-lattice bands". *Proceedings of the Physical Society* **49**, 59 (1937).

[9] N. Bohr. "Studier over Metallernes Elektrontheori", Kobenhavns Universitet (1911).

[10] F. Bloch. "Zur theorie des ferromagnetismus". *Zeitschrift fur Physik* **61**, 206 (1930).

[11] D. van Oosten, P. van der Straten, and H.T.C. Stoof. "Quantum Phases in an Optical Lattice". *Physical Review A* **63**, 053601 (2001).

[12] T. Holstein and H. Primakoff. "Field Dependence of the Intrinsic Domain Magnetization of a Ferromagnet". *Physical Review* **58**, 1098-1113 (1940).

[13] H.T.C Stoof, D.B.M. Dickerscheid and K. Gubbels. *Ultracold Quantum Fields* (Springer and Canopus Publishing Limited, Bristol, 2009), 342-343.

[14] D. Jaksch, C. Bruder, J.I. Cirac, C.W. Gardiner and P. Zoller. *Physical Review Letters* **81**, 3108 (1998).

[15] T. Momoi and K. Totsuka. "Magnetization Plateaus as Insulator-Superfluid Transitions in Quantum Spin Systems". *Physical Review B* **61**, 3231 (2000).